C. R. Physique 16 (2015) 862–873

Contents lists available at ScienceDirect

Comptes Rendus Physique

www.sciencedirect.com

Radio science for connecting humans to information systems / L'homme connecté

Overview of mobile localization techniques and performances of a novel fingerprinting-based method

Aperçu des techniques de localisation de mobiles et performances d'une nouvelle méthode basée sur l'identification d'empreintes

Isabelle Vin, Davy P. Gaillot, Pierre Laly, Martine Liénard *, Pierre Degauque

Lab IEMN/TELICE, University of Lille 1, 59655 Villeneuve d'Ascq cedex, France

ARTICLE INFO

Article history:
Available online 29 October 2015

Keywords:
Localization
Fingerprinting
Polarization diversity
Non-cooperative mode
Multipath component distance
Non-line-of-sight

Mots-clés :
Localisation
Identification d'empreinte
Diversité de polarisation
Mode non coopératif
Multipath component distance
Non-visibilité directe

ABSTRACT

Mobile localization techniques in outdoor environment have been widely studied. In this paper, we consider a specific application related to search and rescue activities or electronic surveillance in urban areas. In this case, the localization must be of high accuracy, on the order of 10 m, despite other constraints related, among others, to non-line-of-sight conditions and non-cooperation with other nearby mobiles or cellular base stations. A brief survey of RF-based localization techniques shows that none of them fully satisfy the desired specifications. A novel approach combining fingerprinting and polarization diversity is then described, its performance being assessed from on-site measurements.

RÉSUMÉ

Dans cet article, on envisage une application spécifique des techniques de localisation radiofréquences pour la surveillance ou la recherche de personnes en environnement urbain. La localisation doit être faite avec une précision importante, de l'ordre de 10 m, en dépit de contraintes liées aux conditions de non-visibilité directe et de non-coopération avec d'autres mobiles. Une revue de l'état de l'art des techniques de localisation montrant qu'aucune d'entre elles ne satisfaisait les spécifications souhaitées, une approche innovante, combinant identification d'empreintes et diversité de polarisation, est proposée. Les performances sont évaluées à partir de simulations et de mesures in situ.

0. Introduction

Accurate localization of mobile phone users in outdoor environment has received considerable attention during this last decade and a wide range of commercial software or applications providing information services to customers has been de-

* Corresponding author.
E-mail address: martine.lienard@univ-lille1.fr (M. Liénard).

http://dx.doi.org/10.1016/j.crhy.2015.10.006
1631-0705/

veloped. Among these applications, let us mention the automatic localization of emergency callers in distress, dialing 911 in North America, to improve the efficiency of rescue services. For example, the U.S. Federal Communications Commission (FCC) requires from the wireless service providers that the accuracy for such localization, based for example on cell identification and triangulation technology, must be within 50 to 300 m. To improve this accuracy, one solution proposed by the Canadian Radio-television and Telecommunication Commission (CRTC) is that the Global Positioning System (GPS) caller's location available in his cell phone, called Mobile Station (MS) in the following, would be automatically transmitted with the emergency call.

In this paper, we treat a special case of surveillance of people potentially dangerous for our society, which is an important item dealing with the security of citizens. Hence, the localization of their mobiles can be an additional tool to the existing techniques used by the teams during surveillance missions. The localization accuracy must be on the order of 10 m despite other constraints related, among others, to the fact that MS is in an urban or suburban environment. The signals between MS and the cellular network base stations (BS) will thus suffer from strong multipath effects, while the probability to be in Non-Line Of Sight (NLOS) scenario is also high. The GPS option cannot be chosen since one can easily imagine that a dangerous individual has disabled the tracking GPS capability of his phone; otherwise he uses a cell phone not having GPS. Note that the same problem occurs to precisely locate not such individuals but an injured person in case he is incapacitated to give a call and whose cell phone has no GPS availability.

The first step of this study was to make an overview of the most relevant techniques already described in the literature and which could be applied, as least in their basic principles, to our application. This is briefly summarized in Section 1 where advantages/disadvantages as well as performances of different techniques are discussed. Since it appears that in NLOS conditions, the aimed accuracy can be reached only with a very large number of BS and with the cooperation of nearby MSs, which is not possible for surveillance applications, a new technique based on a fingerprinting approach has been proposed.

The starting assumption is that the MS was roughly estimated within a hundred-meter radius area with the GSM cell identification approach or any other means. Thus one or a few dedicated receiving stations (RS) can be deployed in this area to detect and process signals sent by the MS without the knowledge of the MS's owner. This can be done owing to an improved and modified version of International Mobile Subscriber Identity (IMSI) catchers, whose description is out of the scope of this paper, acting as a "false" BS, able to force the MS to send messages which will be received by RS. As a result, in such a configuration, MS and RS are not synchronized and the localization is made without the cooperation of possible other nearby cellular phones knowing their positions or of the BSs of the cellular network.

The principle of the method already described in [1] is briefly recalled in Section 2. An improvement of the localization algorithm is proposed by introducing polarization diversity at RS to take into account that the orientation of the MS antenna is unknown. In Section 3, we will focus on experimental results, in order to extract statistics on localization accuracy in real conditions. This is an important concern for the final assessment of a localization method. Indeed, for an urban scenario, characteristics of the propagation paths deduced from simulation or from measurements may sometimes strongly differ, impacting the estimation of the method reliability.

1. Survey of RF-based localization techniques

Most RF ground-based localization techniques rely on the signals transmitted by the MS and received by BSs (or by anchor nodes). For each MS-BS radio link, specific characteristics or signatures as RSS (Received Signal Strength), TOA (Time Of Arrival), TDOA (Time Difference Of Arrival), AOA (Angle Of Arrival), PDP (Power-Delay Profile), are extracted from received signals and used by a dedicated localization algorithm to obtain an estimate of the MS position. Hence, the accuracy and robustness of the procedure is tightly bound to given system parameters and environment in which the MS has to be localized. For example, system parameters include the bandwidth of the signals, the deployment or not of antenna arrays for the MS and/or BS, the number of snapshots collected over time, while the environment is divided into 2 classes: Line Of Sight (LOS) or NLOS. The survey described below does not pretend to be exhaustive, the idea being to extract from the literature a few papers describing techniques having possible application to our localization problem. Generally, localization techniques are split into two categories [2]: geometrical and non-geometrical techniques.

1.1. Geometrical techniques

For this first category, the position is estimated by compiling one or more channel characteristics (AOA, TOA, or RSS) into a geometric output. Equations relating the unknown position of the MS with the known positions of the BSs are derived and solved to estimate the MS position. Optimization routines such as the Least Squares algorithm (LS) are often used as a metric to minimize the estimation error. One could mention:

- The TOA method [3] which requires a perfect synchronization between the MS and BSs, a large bandwidth to obtain a time delay resolution small enough for the desired localization accuracy. Also, the algorithm implicitly needs the knowledge of the LOS TOA. We note this is not always possible and in particular for urban and indoor environments where the MS-BSs links are in NLOS. The NLOS condition adds a positive delay bias to the real TOA and can introduce severe localization errors if it is not corrected or removed with specific treatments as reported in [4,5].

- The TDOA techniques [6,7] rely on the time difference of arrival for signals arriving between all possible BS pairs. Its main advantage is that the synchronization between the MS and BSs is not required even though all BSs must be synchronized. Nevertheless, such techniques do not perform well for NLOS scenarios. Variants have been developed as OTDOA (Observed TDOA) or EOTD (Enhance Observe Time Difference) and applied to LTE (Long term Evolution) broadband technologies [8].
- The AOA techniques [7,9] use the triangulation approach and require at least 2 BSs. Each of them must be equipped with an antenna array to extract AOA of the impinging signals thanks to an estimation algorithm. Information on the AOAs is then sent through the network. There is no need for clock synchronization but the technique suffers from a low accuracy due to the performance of the angular estimator. The variance of the estimation error depends on the antenna array aperture and type of estimation algorithm (spectral or high resolution). Also, the triangulation technique fails for NLOS scenarios. In contrast with TOA and TDOA methods, correction techniques for NLOS scenarios are scarce because the estimated paths do not present prevailing AOA, their directions being distributed between $[-\pi, \pi[$. Alternative solutions do exist to treat NLOS scenarios but are based on hybrid approaches [10,11].
- For TDOA and TOA techniques, strategies to improve localization accuracy in NLOS conditions are highlighted in [4] providing the use of highly dense networks such as indoor sensor networks. One approach consists in identifying and processing all MS-Anchor Nodes links with a LOS and discarding the NLOS ones: this falls under the IAD (Identify and Discard) techniques. For example, the residue algorithm [12,13] was proposed to identify the MS-Anchor Node links with NLOS conditions.
- In RSS techniques, RSS is converted into distance owing to a selected empirical propagation model. The choice of the model is quite critical and depends on the environment type [3]. This is a highly parametric approach leading to inherent difficulties related to model parameters availability, reliability and representativeness. RSS techniques do not require any synchronization between the MS and BSs and are widely popular for LOS scenarios due to their simplicity and cost-effective implementation. For NLOS scenarios, the path loss propagation models are not reliable, which results in degraded performances. Hybrid correction NLOS techniques have been proposed to improve the RSS accuracy by jointly using, for example, AOA and RSS [14].

1.2. Non-geometrical techniques

These techniques do not use lines of position (LOP) deduced from the estimated geometrical characteristics of the (multi)paths, as pseudo distances and AOA, to compute the MS location. One can mention, among others, the approach using cooperative mobiles and the fingerprinting method.

- The precision and coverage of the localization technique can be improved by enabling the cooperation of the MSs (Cooperative Mobiles – CMs) around the MS to be positioned. Hence, MS-BS, CM-BS, and CM-MS links can be distinguished. Note that the cooperative approaches are also practicable with geometrical techniques, relying for example on TOA and/or AOA, and are mentioned in Table 2. Cooperative localization algorithms can be split into two categories: distributed and centralized algorithms for which the measurement data is stored into a dedicated processing unit of the network to compute the MS position [15–17].
- The fingerprinting (FP) or database (DB) correlation techniques are alternatives to geometrical techniques. If all previous techniques are sensitive to the propagation conditions (NLOS, multipath), the FP can be applied to any scenario and environment. In a preliminary step, often called *offline*, the area of interest is discretized into cells and a large DB is built from the channel or signal signatures $fp_i(x_j)$ between each cell of coordinates x_j and the ith BS. The DB can be assembled with measured data or simulated with a propagation simulator. In the *online* step, the estimated signatures $\widehat{fp}_i$ at each BS are compared with the DB fingerprints. The basic concept to deduce the position of the MS is to minimize the Euclidian metric given by (1), where R is the number of BSs:

$$\widehat{x} = \arg\min_{x_j} \left\{ \sum_{i=1}^{R} \left(\widehat{fp}_i - fp_i(x_j) \right)^2 \right\} \tag{1}$$

Table 1 summarizes a few relevant publications on the FP techniques.

It must be emphasized that major drawbacks of FP are associated with database maintenance, sensitivity to environmental changes and cumbersome learning. Improved methods have been developed and are divided in three categories: the deterministic methods as the k-nearest neighbors [6], the probabilistic methods using Bayesian decision frameworks [18] and those integrating statistical training sequences owing to Artificial Neural Networks as in [29]. Furthermore, the offline step is often time consuming, especially if it is based on measurements. Interpolation methods have thus been developed, exploiting the correlation between nearby fingerprint [20]. Other recent research efforts regard blind crowd sourcing for participative database building [22].

1.3. Performance of a few localization techniques

Table 2 presents the best performances of the most recent techniques reported in the literature as well as the conditions at which they have been obtained. In most cases, the authors use the root mean square error (RMSE) and cumulative

Table 1
Few publications on fingerprinting techniques.

Signatures	References	Database from: propagation tool (P) or measured data (M)
RSS	[18–24]	M [18,20–24] P [19]
TOA	[25]	M
RSS + phase and carrier code (GNSS signal)	[26]	M
TDOA	[27]	M
Channel Impulse Response (CIR)	[28,29]	M [29], M or P [28]
CIR/TOA	[30]	M and P
RSS/TDOA	[31]	M
AOA/TDOA	[32,34]	P
PDDP (Power Doppler-Delay Profile)	[33]	M or P

Table 2
Summary of the most recent performances reported in the literature based either on simulation (Sim.) or on experiments (Exp.).

Localization method	Technique	Precision	Environment/scenario	Sim./Exp.	Number of BS, AN or CN
Geometrical	TOA [5]	25 m RMSE (10 m best case)	NLOS 600 m × 600 m urban microcell	Sim.	3 BSs
	LTE OTDOA [8]	92.9% ≤ 50 m 97.2% ≤ 150 m	Outdoor 500 m radius	Sim.	4 BSs
	AOA [9]	RMSE 1 m/10 m, (for 1°/10° angular error standard deviation, respectively)	N/A	Sim.	10 AN
	AOA & RSSI [14]	1.25 m mean error $CDF_{90\%}$ 2 m	LOS 10 m × 10 m indoor (basketball court)	Exp.	2 AN
	Time advance & RSS [35]	Mean error < 5 m	Outdoor	Sim.	7 BSs
Geometrical w/ cooperative nodes	TOA [36]	RMSE 6 m – LOS RMSE 16 m – NLOS	LOS & NLOS 350-m radius	Sim.	14 BSs + 3 to 11 Cooperative nodes
	TOA & AOA [37]	$CDF_{90\%}$ 30 m $CDF_{50\%}$ 15 m	NLOS 100 m radius microcell	Sim.	3BS + 5CN
Fingerprinting	FP-RSS [18]	3 m precision for 82% of cases	21 m × 80 m indoor	Exp.	6 AN
	FP-TDOA [27]	RMSE 1 m	10 m × 10 m indoor	Sim.	10 AN
	FP-Impulse response + TOA [30]	RMSE 0.1 m – LOS RMSE 2.1 m – NLOS	LOS & NLOS 8 m × 6 m indoor	Sim.	4 AN
Cooperative finger printing	FP-RSS GSM+WiFi [20] GSM [21–23]	$CDF_{50\%}$: 30 m	Urban scenario Max. size: 1.3 km radius	Exp.	N/A

distribution function (CDF) of the localization error (in %) to assess the performance of their algorithm. In this table, mobile localization techniques based either on BSs or on anchor nodes (AN) or cooperative nodes (CN) in case of sensor networks, are considered.

For LOS scenarios, the AOA estimate of the LOS can be used to reach a few meters accuracy with algorithms solving inverse problems. Since AOA techniques fail for NLOS scenarios, they are often combined with TOA or TDOA.

For a TOA approach in NLOS urban microcells, a very large number of BSs, as high as 14 mentioned in [36], and with additional cooperative nodes, is needed to get a predicted RMSE accuracy of 16 m. With only 3 BS and TOA measurements, an RMSE of 25 m could be obtained, at least from numerical simulation, by using a fuzzy-tuned hybrid systems technique. However this plausible approach, as stated by Ho in [5], cannot be transposed to our case since it requires modeling the dynamics of MS moving in LOS/NLOS environment.

From this survey, it appears that geometrical methods not allowing one to reach the aimed localization accuracy of about 10 m for our application, a new fingerprinting method using a database combining AOA and TDOA, and polarization diversity has been proposed.

2. Mobile localization technique: a new fingerprinting-based method

2.1. Main features of the proposed method

It is assumed that MS has been roughly localized by any means, typically within an area of a few hundred meters per side. The objective is to reach accuracy on the order of 10 m, in NLOS conditions and without the knowledge of the individual. To achieve this goal, we propose to deploy in the search area a few dedicated RSs able to process signals sent by the MS in order to extract channel characteristics as AOA and TDOA of the various paths between MS and RS. As explained in the introduction, this can be done owing to a system forcing the MS to successively transmit a GSM signal in 110 channels of the GSM band, leading to a concatenated transmitted bandwidth of 22 MHz. Note that MS and RS are not synchronized and that this bandwidth remains much smaller than the band usually needed to reach the desired 10 m localization accuracy.

The method relies on an FP technique by comparing a metric, combining AOAs and TDOAs, whose value is either predicted or deduced from measurements. In the context of punctual and rapid MS localization, a propagation tool must be considered to build the DB. The Digital Elevation Model (DEM) of the environment is assumed to be available from a 3D modeling tool, such as Sketch up or from Google Earth. Therefore, the a-priori known environment is digitalized and divided into a large number of elementary cells. The ray-launching (RL) is used to compute the predicted radio links, and thus the Angle Of Departure (AOD) and TOA, from the known RS positions to all possible positions of the MS in the digital map [38]. This configuration corresponds to a "downlink (DL)". All these values are stored to build the database of the FP. During the localization process, a High-Resolution Algorithm (HRA) extracts the AOA and relative TOA of the most energetic paths of the signal emitted by the MS and received by the RS ("uplink UL"). It must be noted that the predicted AOD (DL) must correspond to the measured AOA (UL) at RS, due to the channel reciprocity. The measured channel signature will be compared with all stored signatures of the database to select the most likely cell in which the MS is located. The elevation angles were discarded from the study since their estimation is not faithful with the horizontal antenna array used in the experimental approach. Nevertheless the extrapolation of the procedure, described hereafter, to the 3-dimensional case is straightforward. It must be emphasized that applying FP is not as simple as appears at first glance, the issues being related to the lack of synchronization between MS and RS and to the approximate prediction of the channel characteristics. Indeed a DEM does not take into account fine details of the environment nor obstacles as cars, fences or metallic stairs. Furthermore the orientation of the MS is unknown and thus the polarization of the transmitting wave.

2.2. Principle of the localization algorithm

After a brief recall on the basic principles of the FP method, details on the analytical formulation being given in [1], the main issues and the proposed solutions are discussed.

The metric used to compare the predicted and estimated paths is based on the Multipath Component Distance [39] in the time domain (MCD_{T}) and angular domain (MCD_{A}). The MCD_{T} between the TOA of the ith UL estimated path, noted $\widehat{ToA_i}$, and the TOA of the jth DL predicted path for the mth cell, noted ToA_j^m, is given by:

$$(MCD_T)_{i,j}^m = \frac{|ToA_j^m - \widehat{ToA_i}|}{\Delta t} \tag{2}$$

In this formula, Δt is the time-delay resolution corresponding to the inverse of the transmitting bandwidth.

Similarly, the MCD_{A} between these two paths is defined by:

$$(MCD_A)_{i,j}^m = \frac{1}{2}\left[\Omega(\widehat{AoA_i}) - \Omega(AoD_j^m)\right] \tag{3}$$

where $\widehat{AoA_i}$ is the estimated AOA of the ith path.

To simplify the presentation, the link is assumed in a horizontal plane (2D approach). In this case, the spatial steering vector Ω of a given ray is expressed as a function of the azimuth φ by:

$$\Omega(\varphi) = [\cos\varphi, \sin\varphi] \tag{4}$$

Note that the extrapolation to the 3D case is straightforward but needs of course an adequate receiving array.

To highlight the issues of the FP method, related to synchronization and accuracy of predicted channel characteristics, Fig. 1 shows an example of the discrete channel impulse response, either predicted by the RL software or estimated from measurements at 1.3 GHz in a 22 MHz bandwidth and by applying HRA named RiMAX [40]. These results have been obtained for one of the links shown in Fig. 2, the experimental approach being described in the next section. Only paths

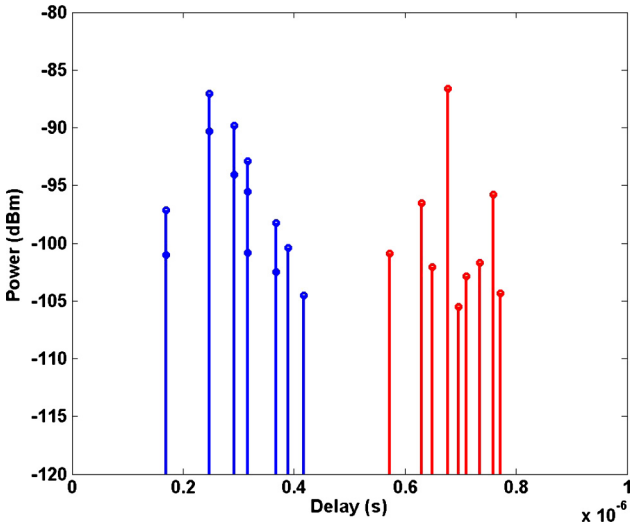

Fig. 1. (Color online.) Estimated (red) and predicted (blue) discrete channel impulse response before applying the synchronization process.

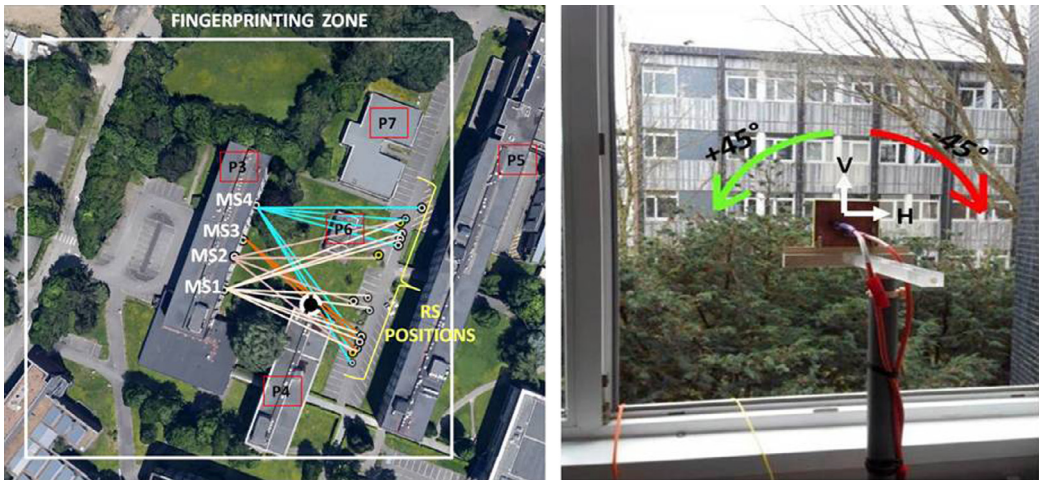

Fig. 2. (Color online.) (a) Top view of the measurement site located on the Lille-1 University Campus. (b) 3 possible orientations of the MS antenna located at point MS1 (polarization H, V or $\pm 45°$).

exhibiting an attenuation less than 20 dB, referred to the most powerful path, have been considered. Even by introducing this threshold for the predicted paths, it appears that the number of paths, amplitude and delays differs according to these two approaches. One of the main reasons arises from the granularity of the DEM and the presence of vehicles and more generally, of any type of obstacles not taken into account in the DEM. The unknown device attitude and the unexpected obstructions induced by the user's body for example, also contribute to discrepancies between predictions and measurements. Furthermore, limitations on the accuracy of the results may also be due to the RL tool which must ensure a compromise between high accuracy and computation time. At this stage, it must be outlined that the objective of this paper is to study the feasibility of the proposed FP technique using commercial RL software and available DEM of the area of the experiments. Therefore no extensive study on the impact of the type of RL and DEM has, for the time being, been carried out.

To cope with these problems, a pairing procedure is first applied between a few powerful predicted paths and estimated paths. Since RS and MS are not synchronized, the pairing procedure must start from results in the angular domain. If we consider any cell m, the two sets of pairs are obtained by searching for the predicted path (index j) which minimizes the MCD_A matrix for each estimated path (index i). They are given by:

$$\left[m, (i, j_i)\right] = \arg\min_j (MCD_{\mathrm{A}})^m_{i,j} \tag{5}$$

It remains to determine the time shift to be applied to the experimental paths. This is done by synchronizing, in each cell, the most likely pair (i_0, j_0) in the angular domain, i.e. minimizing MCD_A:

$$\left[m, (i_0, j_0)\right] = \arg\min_{i,j}(MCD_{\mathrm{A}})^m_{i,j} \tag{6}$$

After this synchronization process, the global metric associated with any cell m, and noted MCD^m, can be calculated. It is defined by (7), as a weighted combination of MCD_{A} and MCD_{T}, the coefficient α balancing their relative contributions:

$$MCD^m = \frac{MCD^m_{\mathrm{A}} + \alpha MCD^m_{\mathrm{T}}}{1+\alpha} \tag{7}$$

The weighting factor α depends on the relative position of the RS and of the MS in the environment. Indeed, in some cases one can find either a strong minimum on the MCD value in the time domain but a wide spread in the angular domain, while in other cases, the contrary may occur. By making a statistical approach, it was found that the optimum value of α can be deduced from the cumulative distribution function of MCD_{A} and MCD_{T}, details being given in [1]. For the configuration described in Section 3 and for the various positions of the MS and RS, the values of α for a probability between 10% and 90% vary from 0.1 to 0.5.

The orientation of the MS antenna and subsequent polarization, noted "u", of the MS signal is unknown. Hence, polarization diversity must be considered at the RS receiving array. This is introduced by deriving a general form of the global metric, $(MCD_{\mathrm{div}})^m$, which includes polarization diversity. Furthermore, additional metrics $(MCD_{\mathrm{uH}})^m$ and $(MCD_{\mathrm{uV}})^m$ which respectively compare the uH and uV measured channels to the HH or VV predicted channels are computed. Let P_{uV} and P_{uH} the sum of the power of the two most powerful paths, for V and H receiving polarization, respectively. To take into account their relative power, a weighting factor α_{pol} is finally introduced yielding:

$$(MCD_{\mathrm{div}})^m = \frac{(MCD_{\mathrm{uV}})^m + \alpha_{\mathrm{pol}}(MCD_{\mathrm{uH}})^m}{1+\alpha_{\mathrm{pol}}} \tag{8}$$

with $\alpha_{\mathrm{pol}} = (P_{\mathrm{uH}}/P_{\mathrm{uV}})$.

The value of α_{pol} is of course strongly dependent on the type of scenario: LOS or NLOS. For the set of measurements described in Section 3, the values of α_{pol} for a probability between 10% and 90% are between 0.02 and 11, with a median value of 0.9.

Here, Eq. (8) applies to the case of a single RS but can be easily generalized to any number K of dedicated RSs deployed in the search area. In this case if $(MCD^k_{\mathrm{div}})^m$ is the metric given by (8) and related to the kth RS, the final metric is given by:

$$(MCD_{\mathrm{final}})^m = \frac{1}{K}\sum_{k=1}^{K}\left(MCD^k_{\mathrm{div}}\right)^m \tag{9}$$

Finally, to estimate the MS position and remove artifacts, a set of lowest $(MCD_{\mathrm{final}})^m$ are selected and the k-Nearest Neighbors method [41,6] is used to estimate MS position by averaging the coordinates of these cells weighted by the inverse of their respective global metric.

3. Experimental assessment of the proposed method

3.1. Experimental set-up

The measurement campaign took place on the Lille-1 University campus (top view shown in Fig. 2). This environment was selected as it hosts all the possible scenarios investigated for the development of the localization method. For instance, it can be classified in-between urban and suburban and is characterized by a large number of buildings which results in numerous reflections, diffractions, and a wide set of NLOS scenarios. In addition, the presence of spread out vegetation has to be highlighted as it provides diffusion and depolarization mechanisms. If vegetation is situated in the LOS of a link, such a link will be noted OLOS (Obstructed LOS).

As shown in Fig. 2a, the P3, P4, and P5 are 16 m three-story high buildings whereas P6 and P7 are only 3 m high. For any considered scenarios, the transmitting antenna, acting as MS, was located at a height of 5.45 m, at one of the P3 1st level windows opened on an outdoor environment where the RSs are situated (Fig. 2b). The receiving antenna array (RS) was outside on the parking at 1.4 m. The positions of MS and RS are indicated with black filled circles with white edges. 4 MS positions (MS1–MS4) were considered. The search area is 142.5 m × 142.5 m (Fig. 2a) divided into 3249 squared cells of 2.5 m side.

In this configuration, the MS being situated at a window, the contribution of the indoor multipath is negligible. Indeed, the objective of the measurements is, in this first step, to assess the localization method assuming propagation in an outdoor environment. If MS is situated in "light indoor" (LI), i.e. in the room facing the search area where the RSs are deployed, most of the transmitting power will propagate through the window and part through the wall of the building closest to the MS, leading to a decrease of the localization accuracy. Of course, for "deep indoor (DI)" this accuracy will strongly depend on

Table 3
Description of the measurement campaign scenarios.

MS POLAR	Number and type of scenarios	Measured channel: uY u: MS polarization Y: RS polarization
H OR V ±45°	2 LOS/5 OLOS/15 NLOS 1 LOS/3 NLOS	HH, VV, HV, VH (45°, V), (45°, H), (−45°, V), (−45°, H)

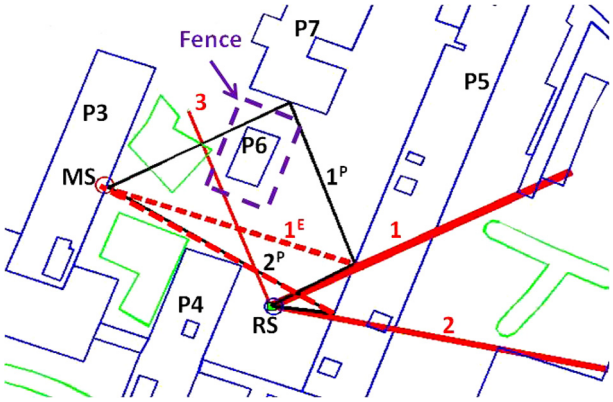

Fig. 3. (Color online.) Top view of the investigated urban site. A few estimated and predicted paths with VV polarization: the red and black solid lines represent the estimated (AOA) and predicted (AOD) paths, respectively.

the structure of the building, on the location of MS and on the presence of obstacles or reflecting surfaces as furniture. An example of the distribution of AOA and AOD in such a configuration is given in [42] for the case of a transmitting antenna being in LOS of the building, the receiving antenna being moved from LI to DI. However, the impact on the position of MS inside the building on localization accuracy has not yet been studied.

The MS transmitting antenna is a patch antenna whose main radiation lobe is oriented towards the free space, i.e. perpendicular to the facade of the building. At RS, a virtual 12-element circular array (UCA) was used. A patch antenna, vertically or horizontally polarized, was thus put on a rotating arm, 18 cm long, measurements being successively made on 12 equally spaced positions.

Measurements have been carried out by considering 4 successive positions of MS (MS1 to MS4) but only a limited number of receiving points. Each pair MS-RS, identified by a line drawn in Fig. 2a corresponds to a LOS, NLOS or OLOS scenario as indicated in Table 3.

The polarization of the MS noted u was selected to be either V, H, or ±45° (Fig. 2b), whereas the polarization of the RS noted Y was V and H.

The channel transfer function uY between MS and each element of the RS-UCA was measured with a Vectorial Network Analyser (VNA) on 1601 frequency points, equally spaced on a 22-MHz bandwidth around 1.3 GHz. Transmitting and receiving antennas were connected to the VNA owing to fiber optics, avoiding the strong attenuation presented by coaxial cables, and by inserting optical/RF converters. The calibration of the VNA includes both cables and converters.

3.2. Channel characteristics in urban environment: from simulation to measurements

As an example, Fig. 3 presents a few estimated (AOA – solid red lines) and predicted (AOD – solid black lines) paths for the one of the links, and for a VV configuration. These paths have been selected to show the discrepancies which may sometimes appear. The thickness and length of the solid red lines correspond to the path amplitude and distance obtained from the estimated TOA, respectively. For instance, the most energetic estimated path labeled "1" in Fig. 3 has the same AOA as the predicted path "1^{P}" resulting in the same interaction point on the P5 building. However, their respective TOA are different. Starting from the interaction point, the reconstructed path having the same TOA as "1" would be "1^{E}". It must be noted that this path "1^{E}" does not correspond to a specular reflection on the building. This effect could be attributed to the geometrical structure of this building which presents vertical beams on its facade. It is noteworthy that some of the estimated paths were not predicted by the RL model. As an example, the metallic fence around the P6 building yields to the non-predicted path "3". Fortunately, such discrepancies between predicted and estimated paths rarely occur and a good agreement is often obtained as shown by paths "2" and "2^{P}". Lastly, both measurements and simulation show that the amplitudes of the paths are different between VV and HH since the complex reflection and diffraction coefficients are polarization dependent.

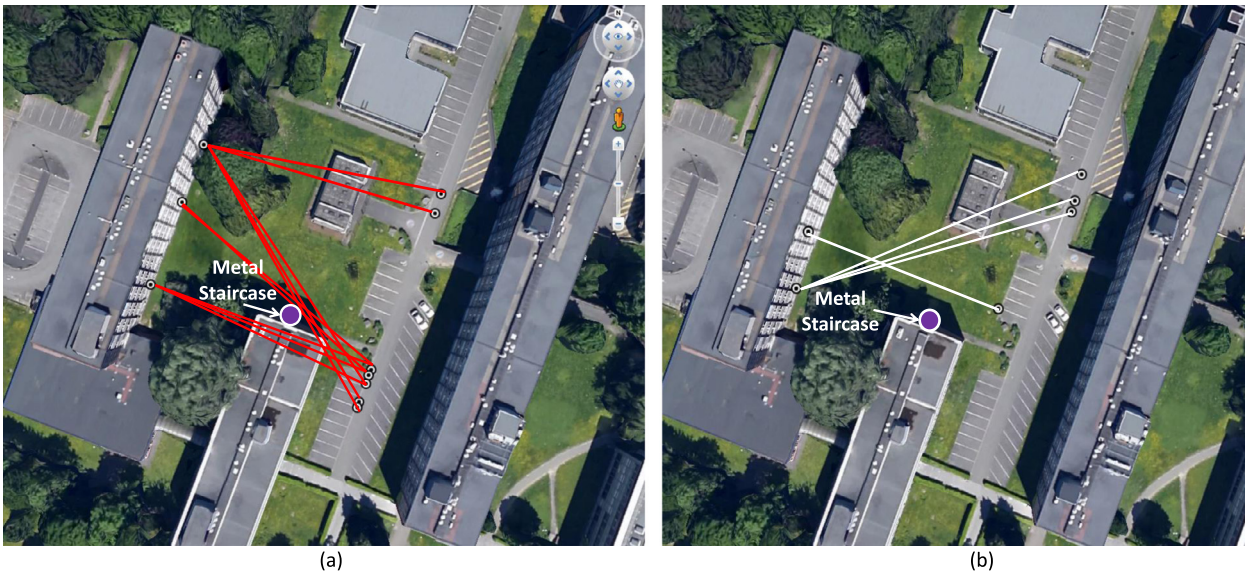

Fig. 4. (Color online.) MS-RS XPD categorization: (a) $0 < \text{XPD} < 7$ dB. (b) $\text{XPD} > 10$ dB.

Table 4
Median values ($\text{CDF}_{50\%}$) of the radio channel characteristics for the experimental and simulated links.

	$P_{\text{mean,HH}}/P_{\text{mean,VV}}$ (dBm)	τ_{RMS} V/H (ns)	θ_{RMS} V/H (°)	$\text{XPD}_{\text{V}}/\text{XPD}_{\text{H}}$ (dB)
Experimental	−49.6/−52	45/49	59/59	7.8/8
Simulation	−45/−48	44/49	48/49	N/A

It is also interesting to deduce from measurements the cross-polar discrimination (XPD) factor defined as the ratio between the mean power of the co-polar and of the cross polar link. This mean power corresponds to the received power averaged over the receiving array. Hence, for an H-polarized transmitting antenna (Tx), XPD_{H} is given by:

$$\text{XPD}_{\text{H}} = \frac{P_{\text{mean,HH}}}{P_{\text{mean,HV}}} \tag{10}$$

A similar formula is obtained for a V-polarized Tx by interchanging V and H.

The values of both XPD_{V} and XPD_{H}, deduced from the 22 scenarios (Table 3) are between 0 and 17 dB. From this analysis, the MS-RS links can be categorized upon the strength of the depolarization mechanism, as shown in Fig. 4. The first category includes the links for which large depolarization mechanisms ($0 < \text{XPD} < 7$ dB) are observed (Fig. 4(a)), while in the second category, the links present weak depolarization mechanisms leading to $\text{XPD} > 10$ dB (Fig. 4(b)). The low XPD values associated with the paths shown in Fig. 4a are attributed either to the presence of an emergency metallic spiral stair or to abundant vegetation in the vicinity of the emitter. In addition to the XPD, the general characteristics of the radio links such as the delay spread (τ_{RMS}) and angular spread (θ_{RMS}) were computed from the estimated and predicted parameters for the 22 VV and HH links. Table 4 presents the experimental and predicted results of the mean received power for a V or H co-polar link and the median values of τ_{RMS} and θ_{RMS}. The last column in Table 4 gives the mean values of XPD_{V} and XPD_{H}. The theoretical received powers were computed from the 22-MHz filtered complex impulse responses. A good agreement is reached between the median values of experimental and predicted characteristics justifying the use of deterministic simulation. Nevertheless, in few cases, discrepancy between predicted and measured paths characteristics may appear, as already shown and explained in the previous section. It is noteworthy that the XPD could not be computed from the RL model since cross-polar links cannot be simulated. Results presented in this table give an idea on the usual channel characteristics encountered in our scenarios, as τ_{RMS} and θ_{RMS}, even if these values have no direct impact on the localization accuracy.

3.3. Performance of the localization algorithm

A simulation has first allowed to test the principle of the method owing to a large number of realizations. For a given position of MS and for VV links, 100 possible positions of RS were envisaged, as described in [43]. For each location of the RS, the FP database is built from the RL software by calculating the channel characteristics (AOD and TOA of the most powerful paths) between this RS and the center of all the 3249 cells of the research area. To simulate results which would

Table 5
Statistical performance of the proposed localization algorithm.

			Proba (%) Error ≤ 10 m	Proba (%) Error ≤ 20 m	Proba (%) Error ≤ 30 m	Proba 50% accuracy (m)	Proba 90% accuracy (m)	RMSE
Simul.	2 RSs	VV	88	96	97	2.5	11.2	11.4
Experimental	w/o polarization	uV	48	75	81	11.2	51.5	27
	diversity – 2 RSs	uH	59	76	82	9	47.8	25.3
	w/ polarization diversity – 2 RSs	u	59	83	89	9	34	19.4
	w/ polarization diversity – 3 RSs	u	71	91	95	7.5	18	14

be deduced from measurements, i.e. for the MS-RS link, the channel transfer function predicted for this link by the RL software is filtered in a 22 MHz bandwidth. The HRA algorithm is then applied by assuming at RS a 12-element uniform circular array, each element being a patch antenna. Finally, the MCD is calculated between the results of the HRA and the FP data.

The statistical results presented in Table 5 have been obtained assuming that two RS are used for the localization, MCD being given by (9). Furthermore, in order to increase the number of realizations, eight positions of the MS were successively considered.

The cumulative localization error below 10 m, 20 m, 30 m, as well as the 50% and 90% accuracy, and root mean square error (RMSE) were computed. All these results are presented in Table 5. The algorithm performance for the theoretical (deterministic) links is with an RMSE of 11.4 m and a probability of 88% to get an error less than 10 m. This error may be explained by: i) the estimation error of the geometrical parameters due to the limited bandwidth and antenna aperture, ii) a synchronization error due to pairing procedure error. Furthermore, since the comparison between predicted and estimated paths is made only on the two or three most powerful paths, artifacts may occur in case of a high degree of similarity between cells signatures. However, the same model being used both for the prediction and the generation of observed signals, experimental results are needed to make a real assessment of the method.

For the experimental part, the algorithm was applied to all available measurements (uV or uH, where u is either H, V, or $\pm 45°$) presented in the previous section. First, without polarization diversity, the performance summarized in Table 5 is observed to be lower with the uV experimental links leading to a 27-m RMSE and a probability of 48% to have an error below 10 m. In contrast, with the diversity-based algorithm, a 19.4-m and 14-m RMSE are obtained with two and three RSs, respectively. In addition, the probability to get an error smaller than 10, 20 or 30 m, is higher with the diversity scheme.

Overall, the results suggest that the diversity scheme improves the performance of the localization approach. Indeed, the orientation of MS being unknown, diversity at RS first avoids the configuration of cross-polarized transmitting/receiving antennas leading to a small signal-to-noise ratio if the waves are not depolarized during their propagation. Furthermore, whatever the polarization of MS, additional data in terms of AOA and TDOA related to the H and V components of the received signal, allows a better evaluation of the MCD, which has a beneficial impact on localization accuracy.

This promising FP method can also fulfill operational constraints as timeliness which is a crucial point for practical security and surveillance application. As soon as MS has been localized in a coarse way using other methods, the DEM of the search area is uploaded on an onboard computer of the RS. Even if this step can take few minutes, this can be done during the deployment of the RS. The final position of RS is chosen on site, depending on the nearby environment and more precisely on the presence of obstacles as trucks or important vegetation. Then running the RL software on a PC takes about 90 s, and the localization algorithm takes a few second or much less depending on the performance of the computer. This time is in line with the requirements for surveillance application.

4. Conclusion

In this work, the state of the art localization techniques of a mobile in urban scenarios were reviewed and discussed. In the special case of precise localization in an urban environment, a new fingerprinting-based localization technique has been proposed and experimentally validated for LOS and NLOS scenarios. The fingerprinting database is built with a RL software which offers the possibility to import maps of the investigated scenarios from Google Earth or via SketchUp. A dedicated metric has been developed to take into account the polarization diversity at the receiver, the polarization of the mobile device being unknown. Despite the fact that the deterministic model does not include realistic details of the environment such as the building facade structure, metallic fences, metallic stairs, cars, or even vegetation, the obtained results are satisfying with a localization error below 10 m for 59% of the measured links with two RSs, while, with three RSs, this probability reaches 71%.

Acknowledgements

This work was supported by the “Agence nationale pour la recherche”, the French Ministry of Research, under contract CSOSG 2010-Gelocom. The authors thank SIRADEL for their kind cooperation on the use of the ray-launching software.

References

[1] I. Vin, D.P. Gaillot, P. Laly, P. Degauque, Multipath component distance-based fingerprinting technique for non-cooperative outdoor localization in NLOS scenarios, IEEE Trans. Antennas Propag. (2014) 4794–4798.
[2] L. Cheng, C. Wu, Y. Zhang, H. Wu, M. Li, C. Maple, A survey of localization in wireless sensor network, Int. J. Distrib. Sens. Netw. (2012) 962523.
[3] F. Seco, A.R. Jimenez, C. Prieto, J. Roa, K. Koutsou, A survey of mathematical methods for indoor localization, in: Proc. 6th IEEE International Symposium on Intelligent Signal Processing, 2009, pp. 9–14.
[4] I. Güvenç, C.C. Chong, A survey on TOA based wireless localization and NLOS mitigation techniques, IEEE Commun. Surv. Tutor. (2009) 107–124.
[5] T.J. Ho, Urban location estimation for mobile cellular networks: a fuzzy-tuned hybrid systems approach, IEEE Trans. Wirel. Commun. (2013) 2389–2399.
[6] H. Lui, H. Darabi, J. Liu, Survey of wireless indoor positioning techniques and systems, IEEE Trans. Syst. Man Cybern., Part C, Appl. Rev. (2007) 1067–1080.
[7] S. Gezici, A survey on wireless position estimation, Wirel. Pers. Commun. (2008) 263–282.
[8] T. Zhang, D. Xiao, J. Cui, X. Lou, A novel OTDOA positioning scheme in heterogeneous LTE-advanced systems, in: Proc. 3rd IEEE International Conference on Network Infrastructure and Digital Content, 2012, pp. 106–110.
[9] Hua-Jie Shao, Xiao-Ping Zhang, Zhi Wang, Efficient closed-form algorithms for AOA based self-localization of sensor nodes using auxiliary variables, IEEE Trans. Signal Process. (2014) 2580–2594.
[10] S. Venkatraman, J. Caffery, Hybrid TOA/AOA techniques for mobile location in non-line-of-sight environments, in: Proc. 2004 IEEE Wireless Communications and Networking Conference, 2004, pp. 274–278.
[11] V.Y. Zhang, A.K.-S. Wong, Combined AOA and TOA NLOS localization with nonlinear programming in severe multipath environments, in: Proc. IEEE Wireless Communications and Networking Conference, 2009, 6 p.
[12] Y.T. Chan, W.Y. Tsui, H.C. So, P.C. Ching, Time-of-arrival based localization under NLOS conditions, IEEE Trans. Veh. Technol. (2006) 17–24.
[13] L. Cong, W. Zhuang, Non-line-of-sight error mitigation in mobile location, in: Proc. 33rd Annual Joint Conference of the IEEE Computer and Communications Societies, INFOCOM 2004, 2004, pp. 560–573.
[14] Jehn-Ruey Jiang, et al., ALRD: AoA localization with RSSI differences of directional antennas for wireless sensor networks, in: Proc. 2012 International Conference on Information Society, 2012, pp. 304–309.
[15] A. Savvides, C.C. Han, M.B. Strivastava, Dynamic fine-grained localization in ad-hoc networks of sensors, in: Proc. IEEE Mobicom, 2001, pp. 166–179.
[16] N. Patwari, J.N. Ash, S. Kyperountas, A.O. Hero, Locating the nodes: cooperative localization in wireless sensor networks, IEEE Signal Process. Mag. (2005) 54–69.
[17] H. Wymeersch, J. Lien, Moe Z. Win, Cooperative localization in wireless networks, Proc. IEEE 97 (2) (2009) 54–69.
[18] Y. Zhao, et al., A novel overlap area matching algorithm based on location fingerprinting in wireless networks, in: Proc. IEEE Wireless Communications and Networking Conference, 2009, 5 p.
[19] J. Baumann, et al., Accuracy estimation of location determination based on database correlation, in: Proc. 2006 International Electric Vehicle Conference, 2006, 5 p.
[20] K. Cujia, et al., DactyLoc: a minimally geo-referenced WiFi+GSM-fingerprint-based localization method for positioning in urban spaces, in: Proc. 2012 Int. Conference on Indoor Positioning and Indoor Navigation, 2012, 9 p.
[21] M. Ibrahim, M. Youssef, CellSense: an accurate energy-efficient GSM positioning system, IEEE Trans. Veh. Technol. (2012) 286–296.
[22] Minkyu Lee, et al., Elekspot: a platform for urban place recognition via crowdsourcing, in: Proc. 2012 IEEE/IPSJ 12th International Symposium on Applications and the Internet, 2012, pp. 190–195.
[23] M.H. Abdel Meniem, A.M. Hamad, E. Shaaban, Relative RSS-based GSM localization technique, in: Proc. 2013 IEEE International Conference on Electro/Information Technology, 2013, 6 p.
[24] Xing-chuan Liu, et al., A real-time algorithm for fingerprint localization based on clustering and spatial diversity, in: Proc. 2010 International Congress on Ultra Modern Telecommunications and Control Systems and Workshops, 2010, pp. 74–81.
[25] B. Li, A. Dempster, C. Rizos, H.K. Lee, A database method to mitigate NLOS error in mobile phone positioning, in: Proc. IEEE Position, Location, and Navigation Symposium, 2006, pp. 173–178.
[26] G. Hejc, J. Seitz, T. Vaupel, Bayesian sensor fusion of Wi-Fi signal strengths and GNSS code and carrier phases for positioning in urban environments, in: Proc. 2014 IEEE/ION Position, Location and Navigation Symposium, 2014, pp. 1026–1032.
[27] H. Jamali-Rad, G. Leus, Sparsity-aware TDOA localization of multiple sources, in: Proc. 2013 IEEE International Conference on Acoustics, Speech and Signal Processing, 2013, pp. 4021–4025.
[28] M. Triki, D.T.M. Slock, V. Rigal, P. François, Mobile terminal positioning via power delay profile fingerprinting: reproducible validation simulations, in: Proc. 2006 IEEE 64th Vehicular Technology Conference, 2006, 5 p.
[29] S. Dayekh, S. Affes, N. Kandil, C. Nerguizian, Radio localization in underground narrow-vein mines using neural networks with in-built tracking and time diversity, in: Proc. 2011 IEEE Wireless Communications and Networking Conference, 2011, pp. 1788–1793.
[30] Md. Humayun Kabir, et al., A hybrid TOA-fingerprinting based localization of mobile nodes using UWB signatures for non-line-of-sight conditions, Sensors (2012) 11187–11204.
[31] W.G. Guan, Z.L. Deng, Y.T. Ge, Y.P. Yu, An indoor location algorithm based on grid characteristic match by TDOA-RSSI, in: MicroNano Devices, Structure and Computing Systems, 2011, pp. 444–449.
[32] B.R. Phelan, E.H. Lenzing, R.M. Narayanan, Source localization using unique characterizations of multipath propagation in an urban environment, in: Proc. 2012 IEEE 7th Sensor Array and Multichannel Signal Processing Workshop, 2012, pp. 189–192.
[33] G. De Angelis, G. Baruffa, S. Cacopardi, GNSS/cellular hybrid positioning system for mobile users in urban scenarios, IEEE Trans. Intell. Transp. Syst. (2013) 313–321.
[34] T. Öktem, D. Slock, Power delay Doppler profile fingerprinting for mobile localization in NLOS, in: 2010 IEEE 21st International Symposium on Personal Indoor and Radio Mobile Communications, 2010, pp. 876–881.
[35] D. Tasseto, et al., A novel hybrid algorithm for passive localization of victims in emergency situations, in: 4th Advanced Satellite Mobile Systems, 2008, pp. 320–327.
[36] Y. Shikur Behailu, T. Weber, Robust cooperative localization in mixed LOS and NLOS environments using TOA positioning, in: Proc. 2014 11th Workshop on Navigation and Communication, 2014, 6 p.

[37] G. Ding, et al., Hybrid TOA/AOA cooperative localization in non-line-of-sight environments, in: Proc. 2012 IEEE 75th Vehicular Technology Conference, 2012, pp. 1–5.
[38] Y. Corre, Y. Lostanlen, Three-dimensional urban EM wave propagation model for radio network planning and optimization over large areas, IEEE Trans. Veh. Technol. (2009) 3112–3123.
[39] N. Czink, et al., Improving clustering performance using multipath component distance, IEEE Electron. Lett. 42 (1) (2006) 44–45.
[40] A. Richter, Estimation of radio channel parameters: models and algorithms, Thesis, Department of Electrical Engineering and Information Technologies, TU Ilmenau, Germany, 2005.
[41] A. Roxin, J. Gaber, M. Wack, A. Nait-Sidi-Moh, Survey on wireless geolocation techniques, in: Proc. 2007 IEEE Globecom Workshops, 2007, 9 p.
[42] I. Vin, D.P. Gaillot, P. Laly, J.M. Molina-Garcia-Pardo, M. Lienard, P. Degauque, Analysis of the polarization on the bidirectional channel characteristics in an outdoor-to-indoor office scenario, in: Proc. 19th International Conference on Circuits, Systems, Communications and Computers, 2015, pp. 53–56.
[43] I. Vin, Algorithme de localisation de mobiles en milieu urbain en mode non coopératif, Thesis, University of Lille-1, France, 2014, pp. 76–78.